

Article

UDC 536.4:519.688

Received: 27.11.2024

 <https://doi.org/10.31489/2025PH2/6-18>

Accepted: 28.02.2025

G. Adyrbekova<sup>1</sup>, P. Saidakhmetov<sup>1</sup>, R. Burganova<sup>2</sup>, I. Piyanzina<sup>2</sup>,  
G. Baiman<sup>1</sup>, G. Baubekova<sup>1</sup>, D. Tayurskii<sup>2</sup>


<sup>1</sup>Department of Physics, M. Auezov South Kazakhstan University, Tauke Khan Ave 5, Shymkent, 160012, Kazakhstan;

<sup>2</sup>Institute of Physics, Kazan Federal University, Kremlyovskaya St. 18, Kazan, 420008, Tatarstan, Russia

**Density functional theory study of azobenzene derivatives  
as potential materials for wettability switching**

In this study, density functional theory (DFT) is employed to analyze the properties of 16 azobenzene derivatives, assessing their potential as wettability switching materials. Inspired by K. Ichimura's 2001 report on azobenzene-modified surface wettability, we explore the impact of photoisomerization-induced changes in molecular dipole moments between *cis* and *trans* configurations of different azobenzene derivatives. In parent azobenzene molecule this process transforms non-polar molecule into a more hydrophilic *cis* form. The control of surface wettability holds immense potential across diverse domains, such as industry, medicine, microbiology, electronics, and materials science. By harnessing this control, we can unlock the potential to create innovative materials, elevate functionality, and boost efficiency. It enables to enhance product performance, improve adhesion, and achieve precision in liquid handling. Our investigation delves into the structural, electronic, and molecular aspects of all studied molecules utilizing the hybrid B3LYP functional with DFT-D3 dispersion correction and a 6-31++G(d, p) basis set, presenting promising azo-type structures for surface wettability manipulation. Two azobenzene derivatives emerge as potential candidates, exhibiting transformations during *cis-trans* photoisomerization — one towards increased hydrophilicity and the other in the opposite direction.

**Keywords:** azobenzene derivative, wettability switching, photoisomerization, dipole moments, *cis-trans* configurations, DFT, B3LYP functional, 6-31++G(d, p) basis set, photoswitchable materials, hydrophilicity

 Corresponding author: Saidakhmetov Pulat, [timpf\\_ukgu@mail.ru](mailto:timpf_ukgu@mail.ru)

*Introduction*

Wettability is a significant property of solids, governing the spreading behavior of liquid drops on a solid surface. This phenomenon is quantified through the measurement of contact angle (CA), classifying surfaces as either hydrophilic or hydrophobic. Superhydrophobic surfaces, of particular interest, are intricately connected to both fundamental science and practical applications.

Examples of superhydrophobic surfaces can be found in nature, namely are observed in various plants and insects. Lotus leaves, for instance, are characterized by their ability to repel water, resulting in a self-cleaning effect, while water striders feature hydrophobic legs to stay above the water surface [1]. This has spurred significant interest in constructing novel bio-inspired hydrophilic or hydrophobic surfaces. The applications of such surfaces are diverse, with notable uses in antifogging, self-cleaning glasses (lotus effect), transparent electronics and nanomedicine [2, 3].

Various methods exist for manipulating wettability of solid surfaces, encompassing temperature gradients, electric fields, chemical surface modification, pH alterations, solvent influences, and light irradiation [1, 4, 5]. Benefiting from a non-contact mode and acting as a precise stimulus, light can be accurately directed to the target region for the controlled manipulation of chemical reactions and physical properties, providing a more elegant design and intelligent control. Materials suitable for light-induced wettability control exhibit two fundamental properties under irradiation: a switch between bistable states and a change in surface energy [6]. Among inorganic compounds, titanium dioxide ( $\text{TiO}_2$ ) stands out, transitioning to a highly hydrophilic state ( $0^\circ$  contact angle for water) under ultraviolet irradiation (UV) [2]. Within the realm of organic compounds, azobenzenes, spiropyrans, and cinnamates are notable, showcasing a typical change in chemical configurations between two states. The advantages of organic compounds over inorganic ones include their amenability to chemical modification, adaptability, and greater reaction diversity [6].

The pioneering work on wettability control of a surface modified with azobenzene was introduced by K. Ichimura [7]. The concept revolves around the photoisomerization of azobenzene during irradiation, transforming the nonpolar *trans*-azobenzene into the polar and more hydrophilic *cis*-azobenzene. Following this discovery, azobenzene and its derivatives underwent extensive examination as the base for molecular switches, developing fabrication of the light-responsive surfaces [8–11]. Subsequent investigations focused on the fundamental aspects of *cis-trans* isomerization, including solvatochromic behavior [12–14], solvent-dependent kinetics, intermolecular and surface interactions, and their effect on wettability switching [15–17].

The present research aims to facilitate the fast and simple design of molecules suitable for creating monolayers and functionalized surfaces with controlled wetting properties, responsive to external light irradiation. Through the analysis of structural, electronic, and molecular properties of 16 azobenzene derivatives using the density functional theory (DFT), we evaluate their potential as materials capable of wettability switching. This endeavor is consistent with the broader goal of improving the understanding and application of photosensitive surfaces to control wetting characteristics individually and effectively.

### Methods

For the properties characterization the *ab-initio* calculations were carried out using the Gaussian 16 [18] program within DFT and hybrid B3LYP30 functional with DFT-D3 dispersion corrections. Additionally, water solvent effect was estimated using polarizable continuum model (PCM). The energies of the structures were calculated with a self-consistent field (SCF) convergence of  $10^{-8}$  a.u. for the density matrix. All structures were optimized using the Berny algorithm [19] with the convergence criteria being a maximum force less than  $45 \times 10^{-5}$  and a rms force less than  $3 \times 10^{-4}$ . We used a 6-31++G(d, p) basis set which is the most appropriate in terms of accuracy and computational time for the determination of electronic properties [20]. Geometry parameters for each structure were free of constraints and allowed to relax during the optimization process.

In contrast, our previous research [21] utilized an older computational scheme, focusing on only seven molecules, several of which are reexamined in this study. This shift not only allows for a more comprehensive understanding of molecular interactions but also highlights the advancements made in computational methodologies. The incorporation of these modern techniques provides a clearer insight into the molecular behaviours in aqueous environments, underscoring the significance and originality of the current findings.

The common structure of studied molecules is presented in Figure and includes the following azobenzene derivatives:

1. Azobenzene as a parent molecule;
2. Azobenzene substituted with electron donating groups  $\text{NH}_2$ ,  $\text{SO}_2\text{-NH}_2$ ,  $\text{N}(\text{CH}_3)_2$ , known as aminoazobenzenes;
3. Azobenzene substituted with electron acceptor groups  $\text{OH}$ ,  $\text{NO}_2$ ,  $\text{CH}_2\text{-CH}_2\text{-OH}$ ,  $\text{F}$ ,  $\text{CF}_3$ ,  $\text{C}_6\text{H}_5$ ;
4. Azobenzene substituted with electron acceptor groups in more, than one positions of hydrogen atoms of a phenyl ring;
5. Azobenzene derivatives of the pseudostilbene type.

These derivatives are essentially modified with an electron acceptor at one end of a phenyl ring and an electron-donating group at the other end of another phenyl ring. This type is commonly referred to as push-pull azobenzene, owing to the intriguing charge transfer that occurs within the molecule.

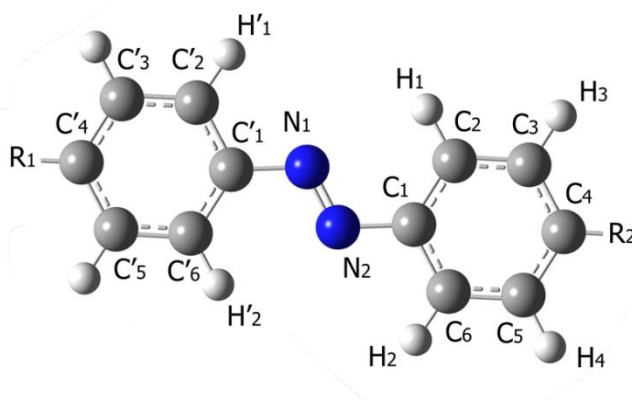


Figure. Structure of *trans* configuration of studied molecules.  
Blue atoms are nitrogen, dark gray atoms are carbon, white atoms are hydrogen

The full list of considered molecules is itemized in Table 1.

Table 1

Short names, functional groups R1 and R2, corresponding SMILES specificities and structural forms of the studied azobenzene derivatives

Short name	R <sub>1</sub>	R <sub>2</sub>	SMILES	The structural formulas of studied compounds
AB	H	H	<chem>c1ccc(cc1)/N=N/c1ccccc1</chem>	
HOAB	OH	H	<chem>Oc1ccc(cc1)/N=N/c1ccccc1</chem>	
FHOAB	OH	F	<chem>Oc1ccc(cc1)/N=N/c1ccc(F)c1</chem>	
CH <sub>3</sub> HOAB	OH	CH <sub>3</sub>	<chem>Cc1cccc(c1)/N=N/c1ccc(O)cc1</chem>	
CH <sub>3</sub> OHOAB	OH	O-CH <sub>3</sub>	<chem>COc1cccc(c1)/N=N/c1ccc(O)cc1</chem>	
CF <sub>3</sub> HOAB	OH	CF <sub>3</sub>	<chem>Oc1ccc(-n:n-c2ccc(cc2)C(F)(F)F)cc1</chem>	
C <sub>6</sub> H <sub>5</sub> HOAB	OH	C <sub>6</sub> H <sub>5</sub>	<chem>Oc1ccc(cc1)/N=N/c1cccc(c1)-c1ccccc1</chem>	
CH <sub>2</sub> CH <sub>2</sub> HOAB	H	CH <sub>2</sub> -CH <sub>2</sub> -OH	<chem>OCCc1ccc(cc1)/N=N/c1ccccc1</chem>	

Continuation of Table 1

Short name	R <sub>1</sub>	R <sub>2</sub>	SMILES	The structural formulas of studied compounds
MY	H	N-(CH <sub>3</sub> ) <sub>2</sub>	<chem>C[n](C):c1ccc(-n:n-c2ccccc2)cc1</chem>	
DO3	NO <sub>2</sub>	NH <sub>2</sub>	<chem>[nH2]:c1ccc(-n:n-c2ccc(cc2)-n(:o):o)cc1</chem>	
AAB	NH <sub>2</sub>	H	<chem>Nc1ccc(-n:n-c2ccccc2)cc1</chem>	
SO <sub>2</sub> NH <sub>2</sub> AB	NH <sub>2</sub>	SO <sub>2</sub> NH <sub>2</sub>	<chem>NS(=O)(=O)c1ccc(-n:n-2ccc(:[nH2])cc2)cc1</chem>	
ADAB	NH <sub>2</sub>	N(CH <sub>3</sub> ) <sub>2</sub>	<chem>CN(C)c1ccc(-n:n-c2ccc(N)cc2)cc1</chem>	
DR1	NO <sub>2</sub>	N(CH <sub>2</sub> CH <sub>3</sub> ) (CH <sub>2</sub> CH <sub>2</sub> OH)	<chem>CC[n](CCO):c1ccc(-n:n-c2ccc(cc2)-n(:o):o)cc1</chem>	

Short name	R <sub>1</sub>	R <sub>2</sub>	Hi	SMILES	The structural formulas of studied compounds
F(HO) <sub>3</sub> AB	F	OH	H' <sub>1</sub> , H' <sub>2</sub> → OH	<chem>Oc1ccc(cc1)/N=N/c1cc(O)c(F)c(O)c1</chem>	
F <sub>5</sub> HOAB	OH	F	H <sub>1</sub> , H <sub>2</sub> , H <sub>3</sub> , H <sub>4</sub> → F	<chem>Oc1ccc(-n:n-c2c(F)c(F)c(F)c(F)c2F)cc1</chem>	
HO <sub>3</sub> AB	OH	OH	H' <sub>1</sub> , H' <sub>2</sub> → OH	<chem>Oc1cc(O)c(-n:n-c2ccccc2)c(O)c1</chem>	

We analyzed both *trans* and *cis* forms, along with all potential arrangements of functional groups for each molecule. Verified stationary configurations were determined through vibrational frequency analysis, exclusively using configurations with real frequencies for calculations. In the case of multiple options, the most stable configuration was chosen for subsequent analysis. Boltzmann statistics were applied to determine the probability and, subsequently, the average value of the desired property for each configuration.

The chemical potential ( $\mu$ ), absolute hardness ( $\eta$ ), and electronegativity ( $\chi$ ) were determined through the finite-difference approximation based on the ionization potential (I) and electron affinity (A). The energy of the last occupied Kohn-Sham orbital corresponds to the highest occupied molecular orbital (HOMO) associated with  $-I$ . Similarly, the energy of the first unoccupied Kohn-Sham orbital is often used as an approximation for the energy of the lowest unoccupied molecular orbital (LUMO) and can be equated with  $-A$ , despite the crude nature of this approximation due to DFT being a ground state theory.

### Results and discussion

#### Optimized structures

The characteristic lengths of bonds, distances, torsion angles, and dihedral angles describing the optimized molecules in their *trans* and *cis* configurations are presented in Table 2.

Table 2

Optimized geometrical parameters (angles in degrees, bond length in Å) for the *trans* and *cis* configurations of studied molecules obtained from B3LYP-D3 6-31++G(d, p) calculations in the gas phase and water solvent

Molecule	<i>trans</i>						<i>cis</i>								
	N1C1	N1N2	N2C1	C4C4	N2N1 C1	N1N2 C1	N1C1	N1N2	N2C1	C4C4	N2N1 C1	N1N2 C1	C1N1 N2C1	N1N2 C1C6	N2N1 C1C2
AB	1.418	1.258	1.417	9.080	115.1	115.1	1.435	1.249	1.435	6.314	123.0	123.0	8.8	50.7	50.7
	1.418	1.259	1.418	9.091	115.4	115.4	1.436	1.252	1.436	6.297	123.0	123.0	9.1	50.8	50.8
HOAB	1.417	1.260	1.411	9.079	115.1	115.3	1.434	1.251	1.431	6.391	123.1	123.6	9.4	42.2	53.9
	1.418	1.261	1.409	9.090	115.2	115.8	1.435	1.254	1.429	6.377	123.1	123.7	9.8	41.8	53.8
FHOAB	1.409	1.260	1.417	9.081	115.5	114.8	1.429	1.251	1.434	6.403	123.7	123.2	9.3	55.1	40.8
	1.407	1.261	1.417	9.092	115.9	115.0	1.427	1.254	1.435	6.400	123.9	123.1	9.6	55.4	39.7
CH <sub>3</sub> HOAB	1.411	1.260	1.418	9.071	115.3	115.1	1.432	1.252	1.434	6.345	123.5	123.1	9.2	53.7	42.2
	1.410	1.261	1.418	9.082	115.7	115.3	1.429	1.255	1.435	6.333	123.7	123.1	9.7	53.2	41.8
CH <sub>3</sub> OHOAB	1.411	1.260	1.417	9.070	115.3	115.1	1.432	1.252	1.435	6.287	123.3	123.0	9.0	51.5	44.6
	1.409	1.262	1.418	9.080	115.9	115.2	1.429	1.255	1.436	6.332	123.7	123.1	9.5	52.7	41.6
CF <sub>3</sub> HOAB	1.408	1.260	1.418	9.066	115.5	114.7	1.428	1.251	1.431	6.379	123.5	123.2	9.3	57.1	57.1
	1.406	1.262	1.418	9.072	115.9	114.9	1.425	1.254	1.433	6.380	123.7	123.2	9.8	40.3	39.2
C <sub>6</sub> H <sub>5</sub> HOAB	1.411	1.259	1.418	9.072	115.3	115.0	1.434	1.252	1.436	6.148	122.8	122.5	8.0	48.1	48.1
	1.409	1.261	1.418	9.082	115.8	115.2	1.431	1.255	1.436	6.206	123.2	122.7	8.7	48.6	45.6
CH <sub>2</sub> CH <sub>2</sub> HOAB	1.418	1.258	1.416	9.101	115.1	115.2	1.435	1.250	1.434	6.327	123.0	123.0	9.0	49.2	51.2
	1.418	1.259	1.416	9.111	115.4	115.5	1.436	1.252	1.433	6.316	122.9	123.0	9.3	48.6	51.9
MY	1.417	1.263	1.403	9.121	114.9	115.7	1.432	1.255	1.423	6.487	123.2	124.2	10.0	35.8	56.5
	1.416	1.268	1.397	9.137	115.0	116.4	1.433	1.262	1.413	6.542	123.1	125.2	10.4	29.7	58.9
DO3	1.397	1.265	1.413	9.060	115.9	114.4	1.418	1.254	1.422	6.493	124.0	124.1	11.0	59.1	32.2
	1.386	1.273	1.408	9.065	116.6	114.3	1.406	1.261	1.418	6.574	124.7	124.5	12.8	59.2	26.6
AAB	1.417	1.262	1.406	9.101	114.9	115.6	1.433	1.253	1.427	6.458	123.2	124.0	9.7	38.0	55.6
	1.417	1.266	1.399	9.119	115.1	116.4	1.434	1.259	1.419	6.497	123.1	123.7	10.3	33.3	57.4
SO <sub>2</sub> NH <sub>2</sub> AB	1.401	1.263	1.416	9.069	115.8	114.5	1.421	1.254	1.427	6.455	124.2	123.5	9.8	59.3	33.1
	1.392	1.269	1.414	9.077	116.5	114.5	1.411	1.260	1.427	6.517	124.9	123.6	10.9	60.1	29.1
ADAB	1.408	1.264	1.406	9.143	115.3	115.5	1.430	1.256	1.427	6.510	123.5	123.7	11.2	42.8	45.8
	1.407	1.269	1.402	9.165	115.7	116.1	1.427	1.263	1.421	6.564	123.7	124.3	12.4	38.7	44.8
DR <sub>1</sub>	1.409	1.259	1.419	9.023	115.4	114.9	1.430	1.251	1.436	6.334	123.7	122.9	9.2	55.8	41.6
	1.408	1.261	1.419	9.037	115.8	115.1	1.427	1.254	1.437	6.344	124.0	122.9	9.5	55.3	40.0
F(HO) <sub>3</sub> AB	1.409	1.259	1.419	9.023	115.4	114.9	1.430	1.251	1.436	6.334	123.7	122.9	9.2	55.8	41.6
	1.408	1.261	1.419	9.037	115.8	115.1	1.427	1.254	1.437	6.344	124.0	122.9	9.5	55.3	40.0
F <sub>3</sub> HOAB	1.405	1.264	1.403	9.106	114.8	116.1	1.419	1.250	1.439	6.412	123.6	122.2	9.4	62.5	40.8
	1.403	1.266	1.402	9.116	115.2	116.2	1.413	1.255	1.436	6.502	124.7	122.6	9.5	60.8	35.3
HO <sub>3</sub> AB	1.410	1.276	1.372	9.078	116.7	117.5	1.425	1.260	1.404	6.892	122.9	128.8	11.0	36.2	49.6
	1.410	1.276	1.373	9.079	116.8	117.3	1.428	1.261	1.405	6.833	122.8	128.2	10.6	37.8	49.3

First, it is noteworthy to highlight that the geometry optimization of the molecules under investigation resulted in all the *trans* configurations being planar, as expected, with dihedral angles C1N1N2C1, N1N2C1C6, N2N1C1C2 equal to 180 degrees.

Upon analysis of the N1N2 bond lengths, we observed that the smallest values were found in the AB and CH<sub>2</sub>CH<sub>2</sub>HOAB molecules. Specifically, the *trans* forms of these molecules exhibited N1N2 bond lengths of 1.258 Å in the gas phase and 1.259 Å in the presence of the water solution model. These bond lengths slightly decreased for *cis* configurations of the molecules to 1.249 Å for the gas phase and 1.252 Å in case of accounting water solution.

Dihedral angles C'1N1N2C1 of *cis* forms of studied molecules range from 8.0 to 11.9 degrees in the gas phase and 8.7 to 14.3 degrees in case of accounting PCM. These minimal and maximal angle values correspond to C<sub>6</sub>H<sub>5</sub>HOAB and DR<sub>1</sub> respectively.

The C1C6 distances, characterizing relative size of a molecule, are changing in case of *trans* conformation from 9.023 to 9.143 Å in the gas phase and from 9.037 to 9.165 Å in case of accounting water solution in calculations. These values exhibited by F(HO)<sub>3</sub>AB and ADAB respectively. For the *cis* conformation C1C6 distances range from 6.148 to 6.892 Å in the gas phase and from 6.206 to 6.833 Å case of accounting PCM in calculations. Corresponding to these extreme cases molecules are C<sub>6</sub>H<sub>5</sub>HOAB and HO<sub>3</sub>AB.

*Energy*

The difference in Gibbs free energies between *trans* and *cis* configurations  $\Delta G$  and corresponding equilibrium constants  $K$  of studied molecules are given in Table 3.

Table 3

**Calculated Gibbs free energy differences  $\Delta G$  (kJ/mole) and equilibrium constants  $K$  between *trans* and *cis* configurations of the most stable conformations of the molecules studied obtained from B3LYP-D3 6-31++G(d, p) calculations in the gas phase and water solvent**

Molecule	$\Delta G$	$K$	Molecule	$\Delta G$	$K$
AB	-55.55	$5.39 \times 10^9$	DO3	-57.43	$1.15 \times 10^{10}$
	-52.45	$1.54 \times 10^9$		-51.69	$1.14 \times 10^9$
HOAB	-57.61	$1.24 \times 10^{10}$	AAB	58.44	$1.73 \times 10^{10}$
	-49.65	$4.98 \times 10^8$		-51.52	$1.06 \times 10^9$
FHOAB	-58.88	$2.07 \times 10^{10}$	SO <sub>2</sub> NH <sub>2</sub> AB	-55.31	$4.91 \times 10^9$
	-52.96	$1.90 \times 10^9$		-49.99	$5.74 \times 10^8$
CH <sub>3</sub> HOAB	-57.23	$1.06 \times 10^{10}$	ADAB	-61.58	$6.14 \times 10^{10}$
	-50.80	$7.93 \times 10^8$		-57.65	$1.26 \times 10^{10}$
CH <sub>3</sub> OHOAB	-56.51	$7.95 \times 10^9$	DR1	-55.94	$6.31 \times 10^9$
	-49.37	$4.45 \times 10^8$		-51.20	$9.32 \times 10^8$
CF <sub>3</sub> HOAB	-59.49	$2.65 \times 10^{10}$	F(HO) <sub>3</sub> AB	-58.43	$1.72 \times 10^{10}$
	-50.23	$6.30 \times 10^8$		-50.44	$6.86 \times 10^8$
C <sub>6</sub> H <sub>5</sub> HOAB	-53.09	$2.00 \times 10^9$	F <sub>5</sub> HOAB	-44.30	$5.77 \times 10^7$
	-45.58	$9.66 \times 10^7$		-32.41	$4.76 \times 10^5$
CH <sub>2</sub> CH <sub>2</sub> HOAB	-55.41	$5.10 \times 10^9$	HO <sub>3</sub> AB	-92.39	$1.54 \times 10^{16}$
	-59.99	$3.23 \times 10^{10}$		-85.41	$9.20 \times 10^{14}$
MY	-57.40	$1.14 \times 10^{10}$			
	-51.32	$9.78 \times 10^8$			

The equilibrium constants were obtained using the formula:

$$K = \exp(-\Delta G / RT), \quad (1)$$

in which the  $\Delta G$  is the difference in the Gibbs energies between *trans* and *cis* configurations,  $T$  is the room temperature equal to 298.15 K and  $R$  is the gas constant.

As expected, the *trans* configurations of all molecules have been found to be more stable than the *cis* configurations, with a stability difference ranging from 44.30 to 92.39 kJ/mol. This is evident from the values of the equilibrium constants, which show a significant difference in magnitude ranging from  $5.77 \times 10^7$  to  $1.54 \times 10^{16}$ . The solvent effect is observed as decrease in Gibbs free energy differences and equilibrium constants with  $\Delta G$  ranging between 32.41 and 85.41 kJ/mol and  $K$  between  $4.76 \times 10^5$  and  $9.20 \times 10^{14}$ , correspondingly.

Based on our calculations, it has been determined that the molecules C<sub>6</sub>H<sub>5</sub>HOAB and F<sub>5</sub>HOAB exhibit the smallest values of Gibbs free energy differences and equilibrium constants. Conversely, CH<sub>2</sub>CH<sub>2</sub>HOAB and HO<sub>3</sub>AB exhibit the highest values of these parameters.

*Electronic properties*

It is well known that the dipole moment of molecules is determined by the formula:

$$p = p_0 + \alpha E + \frac{1}{2} \beta E E + \dots, \quad (2)$$

in which  $p_0$  is the dipole moment without electric field,  $\alpha$  is the second-order tensor of the polarizability and  $\beta$  is the first term in infinite series of hyperpolarizabilities. The polarizability tensor has been diagonalized and afterwards the mean and anisotropic polarizabilities have been obtained using the following formulas:

$$\alpha_{mean} = \frac{1}{3}(\alpha_{xx} + \alpha_{yy} + \alpha_{zz}), \quad (3)$$

$$\alpha_{anis} = \sqrt{\frac{(\alpha_{xx} - \alpha_{yy})^2 + (\alpha_{yy} - \alpha_{zz})^2 + (\alpha_{xx} - \alpha_{zz})^2}{2}}, \quad (4)$$

in which  $\alpha_{xx}$ ,  $\alpha_{yy}$ ,  $\alpha_{zz}$  are the diagonal elements of the polarizability matrix.

All the computed values for dipole moments their differences between the *trans* and *cis* configurations of the most stable conformations of the molecules under investigation are summarized in Table 4, besides, corresponding mean and anisotropic polarizabilities are listed in Table 5. As expected, the calculations accounting a water solvent yielded larger values compared to those obtained in the gas phase, as water serves as a more polarized medium.

Table 4

**Calculated dipole moments  $\mu$  (Debye), their differences between the *trans* and *cis* configurations of the most stable conformations of the studied molecules obtained from B3LYP-D3 6-31++G(d, p) calculations in the gas phase and water solvent**

Molecule	$\mu_{trans}$	$\mu_{cis}$	$\Delta\mu$	Molecule	$\mu_{trans}$	$\mu_{cis}$	$\Delta\mu$
AB	0.00	3.45	3.45	DO3	10.34	7.41	-2.93
	0.00	4.72	4.72		15.61	10.57	-5.04
HOAB	1.65	3.37	1.75	AAB	3.10	5.16	2.06
	2.28	4.76	2.48		5.51	7.70	2.19
FHOAB	2.04	2.51	0.46	SO <sub>2</sub> NH <sub>2</sub> AB	8.03	3.47	-4.55
	2.73	3.54	0.81		12.25	4.99	-7.25
CH <sub>3</sub> HOAB	1.13	3.67	2.54	ADAB	1.35	6.24	4.89
	1.60	5.23	3.63		2.41	9.00	6.59
CH <sub>3</sub> OHOAB	2.84	2.51	0.46	DR1	9.99	7.21	-2.79
	4.05	5.49	1.43		15.36	10.49	-4.87
CF <sub>3</sub> HOAB	4.97	3.05	-1.92	F(HO) <sub>3</sub> AB	1.53	3.81	2.28
	6.28	4.20	-2.07		2.03	5.35	3.32
C <sub>6</sub> H <sub>5</sub> HOAB	1.56	4.30	2.75	F <sub>5</sub> HOAB	4.27	4.50	0.23
	2.17	6.08	3.92		5.10	5.97	0.87
CH <sub>2</sub> CH <sub>2</sub> HOAB	1.53	2.48	0.95	HO <sub>3</sub> AB	2.06	2.34	0.28
	1.92	5.38	3.46		2.88	3.22	0.34
MY	4.28	6.38	2.10				
	6.71	9.58	2.87				

As part of our endeavor to create materials with the ability to switch their wettability under light exposure, we are particularly interested in molecules that exhibit a substantial difference in dipole moments between their *trans* and *cis* forms. The presence of a non-zero dipole moment indicates a polar molecule. When the magnitude of this dipole moment decreases, the dipole-dipole interaction between the molecule and water molecules also diminishes. Consequently, this reduction in interaction leads to a less hydrophilic state in terms of wettability.

Table 5

**Calculated mean and anisotropic polarizabilities  $\alpha$ , and their differences between the *trans* and *cis* configurations of the most stable conformations of the studied molecules obtained from B3LYP-D3 6-31++G(d, p) calculations in the gas phase and water solvent**

Molecule	$\alpha_{trans}^{mean}$	$\alpha_{trans}^{anis}$	$\alpha_{cis}^{mean}$	$\alpha_{cis}^{anis}$	$\Delta\alpha^{mean}$	$\Delta\alpha^{anis}$
AB	183.13	202.86	157.90	79.61	25.22	123.25
	255.20	279.02	221.89	102.05	33.31	176.98
HOAB	194.94	231.47	166.95	95.83	27.99	135.63
	274.31	326.19	235.82	125.87	38.49	200.32
FHOAB	195.56	233.55	166.80	93.94	28.76	139.61
	274.34	330.21	234.56	124.91	39.78	205.30
CH <sub>3</sub> HOAB	209.76	240.00	178.98	87.34	30.79	152.66
	332.76	292.85	253.00	119.62	39.85	213.15
CH <sub>3</sub> OHOAB	214.88	233.15	182.13	80.16	32.75	152.99
	301.28	331.79	259.11	117.96	42.17	213.83

Continuation of Table 5

Molecule	$\alpha_{trans}^{mean}$	$\alpha_{trans}^{anis}$	$\alpha_{cis}^{mean}$	$\alpha_{cis}^{anis}$	$\Delta\alpha^{mean}$	$\Delta\alpha^{anis}$
CF <sub>3</sub> HOAB	213.58	256.98	181.45	97.03	32.13	159.95
	295.52	350.02	252.94	125.42	42.58	224.60
C <sub>6</sub> H <sub>5</sub> HOAB	278.39	295.65	235.08	107.25	43.30	188.40
	384.30	385.50	338.41	157.26	45.89	228.23
CH <sub>2</sub> CH <sub>2</sub> HOAB	220.39	244.29	190.94	99.29	29.45	145.00
	300.78	315.35	262.30	113.86	38.48	201.50
MY	247.59	311.68	209.27	132.92	38.32	178.76
	364.42	483.67	306.23	204.87	58.19	278.80
DO3	251.40	359.38	207.66	138.99	43.73	220.39
	417.03	693.03	319.65	233.22	97.38	459.81
AAB	209.33	261.61	177.46	108.02	31.87	153.60
	311.10	416.70	258.48	160.95	52.62	255.75
SO <sub>2</sub> NH <sub>2</sub> AB	258.47	326.97	217.91	130.69	40.57	196.28
	378.18	499.48	313.64	179.70	64.54	319.78
ADAB	272.01	365.74	225.31	143.98	46.69	221.75
	404.38	573.73	335.62	227.97	68.77	345.76
DR1	328.69	446.52	274.75	179.75	53.94	266.76
	534.16	845.84	418.08	300.55	116.08	545.29
F(HO) <sub>3</sub> AB	206.37	242.27	176.38	95.62	29.99	146.66
	287.45	334.48	247.43	126.17	40.02	208.31
F <sub>5</sub> HOAB	198.14	236.05	169.21	92.11	28.92	143.94
	280.14	354.14	237.49	135.39	42.65	218.75
HO <sub>3</sub> AB	211.78	257.44	181.57	131.85	30.22	125.59
	300.51	368.79	259.57	174.61	40.95	194.18

The *trans* configuration of AB displayed the smallest dipole moment, measuring 0 Debye, which is consistent with its symmetrical molecular structure. Among the azobenzene derivatives, CH<sub>3</sub>HOAB and ADAB exhibited the smallest dipole moments of 1.13 and 1.35 Debye, respectively, in the gas phase. In the water solvent model, these values increased to 1.60 and 2.41 Debye. It is noteworthy that these relatively small dipole moments can be attributed to the compensating effects of the substituted functional groups.

Nevertheless, the ADAB molecule exhibited the most substantial difference in dipole moments between *cis-trans* configurations, surpassing that of AB. This difference amounted to 4.89 Debye in the gas phase and 6.59 when considering water solvent in calculations, compared to 3.45 and 4.72 Debye for AB. Notably, CH<sub>3</sub>HOAB and C<sub>6</sub>H<sub>5</sub>HOAB molecules can be also taken into account as the ones switching wettability from more to less hydrophilic states, with  $\Delta\mu$  values for *cis-trans* configurations equal to 2.54 and 2.75 Debye, respectively, increasing to 3.63 and 3.92 Debye in the water solvent model.

It is crucial to highlight instances of negative differences in dipole moments for DO3, DR1, and SO<sub>2</sub>NH<sub>2</sub>AB. This suggests that the *cis-trans* transition may conversely result in a more hydrophilic state. Particularly noteworthy is the case of SO<sub>2</sub>NH<sub>2</sub>AB, exhibiting the highest negative difference in dipole moments compared to AB, with  $-\Delta\mu$  values of 4.55 and 7.25 in the gas phase and water solvent model calculations, respectively.

Spectroscopic methods offer a means to determine the components of the polarizability matrix. However, obtaining such data can be challenging due to the demanding experimental procedures, particularly for molecules with low or no symmetry. This is where molecular modeling calculations can prove invaluable in fulfilling this objective.

According to our computations, molecules exhibiting the lowest mean polarizability differences include HOAB, F<sub>5</sub>HOAB and HO<sub>3</sub>AB, with respective values of 27.99, 28.76 and 30.22 au in the gas phase, and 38.49, 39.78 and 40.95 au when considering water solvent in calculations. These values contrast with AB, which registers at 25.22 and 33.31 au, respectively. The corresponding anisotropic polarizability differences for these molecules are 135.63, 139.61, and 125.59 au in the gas phase, and 200.32, 205.30, and 194.18 au when water solvent is considered, compared to AB with values of 123.25 and 176.98 au.

Conversely, molecules with the highest mean polarizability differences include DO3, DR1 and ADAB, exhibiting values of 43.73, 53.94 and 46.69 au in the gas phase, and 97.38, 116.08 and 68.77 au when con-



sidering water solvent. The corresponding anisotropic polarizability differences for these molecules are 220.39, 266.76, and 221.75 au in the gas phase, and 459.81, 545.29, and 345.76 au when accounting for water solvent in calculations.

### Molecular properties

In the present work we have obtained the energy of the highest occupied molecular orbital (HOMO) and the energy of the lowest unoccupied molecular orbital (LUMO) as the frontier orbitals of chemical compounds play a vital role in determining their reactivity [22]. It is noteworthy that molecules with a higher HOMO value possess the ability to donate electrons to acceptor molecules with low energy and empty molecular orbitals. Table 6 showcases the calculated HOMO and LUMO energies for studied azobenzene derivatives. Notably, the *trans* and *cis* configurations of the ADAB molecule exhibit the highest HOMO and LUMO values.

Table 6

**Calculated molecular properties of *trans* and *cis* configurations of the studied molecules obtained from B3LYP-D3 6-31++G(d, p) calculations in the gas phase and water solvent. Values are in eV**

Molecule	<i>trans</i>						<i>cis</i>					
	HOMO	LUMO	$\Delta$ LUMO –HOMO	$\mu$	$\eta, \tau$	$\chi$	HOMO	LUMO	$\Delta$ LUMO –HOMO	$\mu$	$\eta, \tau$	$\chi$
AB	–6.46	–2.54	3.93	–4.50	1.96	4.50	–6.06	–2.29	3.77	–4.18	1.89	4.18
	–6.60	–2.73	3.87	–4.66	1.94	4.66	–6.27	–2.48	3.79	–4.37	1.89	4.37
HOAB	–6.11	–2.39	3.72	–4.25	1.86	4.25	–5.86	–2.19	3.68	–4.02	1.84	4.02
	–6.23	–2.60	3.63	–4.41	1.81	4.41	–6.04	–2.40	3.64	–4.22	1.82	4.22
FHOAB	–6.27	–2.59	3.68	–4.43	1.84	4.43	–6.04	–2.36	3.68	–4.20	1.84	4.20
	–6.31	–2.72	3.59	–4.51	1.79	4.51	–6.14	–2.50	3.65	–4.32	1.82	4.32
CH <sub>3</sub> HOAB	–6.05	–2.33	3.72	–4.19	1.86	4.19	–5.81	–2.14	3.68	–3.98	1.84	3.98
	–6.19	–2.57	3.62	–4.38	1.81	4.38	–6.01	–2.38	3.63	–4.19	1.82	4.19
CH <sub>3</sub> OHOAB	–6.00	–2.38	3.61	–4.12	1.81	4.19	–5.86	–2.21	3.65	–4.03	1.82	4.03
	–6.14	–2.61	3.54	–4.31	1.77	4.38	–6.02	–2.41	3.60	–4.22	1.80	4.22
CF <sub>3</sub> HOAB	–6.14	–2.61	3.54	–4.31	1.77	4.38	–6.02	–2.41	3.60	–4.22	1.80	4.22
	–6.38	–2.83	3.55	–4.60	1.78	4.60	–6.21	–2.58	3.64	–4.40	1.82	4.40
C <sub>6</sub> H <sub>5</sub> HOAB	–6.09	–2.40	3.68	–4.25	1.84	4.25	–5.90	–2.24	3.66	–4.07	1.83	4.07
	–6.21	–2.62	3.59	–4.41	1.80	4.41	–6.04	–2.44	3.60	–4.24	1.80	4.24
CH <sub>2</sub> CH <sub>2</sub> HOAB	–6.37	–2.51	3.86	–4.44	1.93	4.44	–6.02	–2.27	3.74	–4.14	1.87	4.14
	–6.50	–2.70	3.80	–4.60	1.90	4.60	–6.18	–2.45	3.74	–4.32	1.87	4.32
MY	–5.38	–2.09	3.29	–3.73	1.65	3.73	–5.33	–1.90	3.44	–3.62	1.72	3.62
	–5.46	–2.41	3.05	–3.93	1.52	3.93	–5.46	–2.21	3.26	–3.83	1.63	3.83
DO3	–6.13	–3.12	3.01	–4.62	1.50	4.62	–6.06	–2.96	3.11	–4.51	1.55	4.51
	–5.90	–3.34	2.56	–4.62	1.28	4.62	–5.90	–3.17	2.73	–4.54	1.37	4.54
AAB	–5.68	–2.19	3.48	–3.93	1.74	3.93	–5.56	–2.00	3.56	–3.78	1.78	3.78
	–5.66	–2.43	3.23	–4.04	1.62	4.04	–5.71	–2.27	3.44	–3.99	1.72	3.99
SO <sub>2</sub> NH <sub>2</sub> AB	–5.97	–2.63	3.34	–4.30	1.67	4.30	–5.87	–2.36	3.50	–4.12	1.75	4.12
	–5.87	–2.77	3.10	–4.32	1.55	4.32	–5.86	–2.50	3.36	–4.18	1.68	4.18
ADAB	–5.02	–1.80	3.22	–3.41	1.61	3.41	–5.01	–1.72	1.53	–0.95	0.77	0.95
	–5.17	–2.19	2.99	–3.68	1.49	3.68	–5.17	–2.12	1.93	–1.16	0.97	1.16
DR1	–5.91	–3.09	2.81	–4.50	1.41	4.50	–5.72	–2.88	2.84	–4.30	1.42	4.30
	–5.69	–3.32	2.37	–4.51	1.19	4.51	–5.63	–3.15	2.48	–4.39	1.24	4.39
F(HO) <sub>3</sub> AB	–6.15	–2.46	3.70	–4.31	1.85	4.31	–5.95	–2.25	3.70	–4.10	1.85	4.10
	–6.23	–2.64	3.59	–4.43	1.79	4.43	–6.07	–2.44	3.63	–4.26	1.82	4.26
F <sub>5</sub> HOAB	–6.58	–2.94	3.64	–4.76	1.82	4.76	–6.55	–2.79	3.76	–4.67	1.88	4.67
	–6.45	–2.97	3.48	–4.71	1.74	4.71	–6.47	–2.81	3.66	–4.64	1.83	4.64
HO <sub>3</sub> AB	–6.16	–2.72	3.44	–4.44	1.72	4.44	–6.03	–2.55	3.48	–4.29	1.74	4.29
	–6.19	–2.75	3.44	–4.47	1.72	4.47	–6.13	–2.64	3.49	–4.38	1.74	4.38

In accordance with Ref. [23] there is a linear correlation between an ionization potential (IP), an electron affinity (EA) and frontier orbitals: HOMO is associated with IP, LUMO can be equated with EA. To

explore the connection between chemical quantities and molecular properties, chemical potential  $\mu$ , absolute hardness  $\eta$ , the first electronic excitation energy  $\tau$  and electronegativity  $\chi$  were evaluated using following formulas [22, 23]:

$$\eta = (E_{LUMO} - E_{HOMO}) / 2, \quad (5)$$

$$\chi = -(E_{LUMO} + E_{HOMO}) / 2, \quad (6)$$

$$\mu = (E_{LUMO} + E_{HOMO}) / 2, \quad (7)$$

$$\tau = \eta, \quad (8)$$

The results of our calculations are collected in Table 6. According to chemical potential values, that are smaller for *trans* configurations of all molecules, than for *cis*, molecules are tending to transit from *cis* to *trans* configuration, that is in accordance with Gibbs free energy results, showing the *trans* isomerization is more stable.

The concept of hardness in the context of molecular systems is closely linked to reactivity. Specifically, a system with a higher value of absolute hardness  $\eta$  tends to exhibit lower reactivity compared to a system with a lower value [22]. Our findings indicate that the molecules AB and CH<sub>2</sub>CH<sub>2</sub>HOAB display relatively lower reactivity, suggesting that they are less prone to undergo chemical reactions. On the other hand, the molecules DO3, DR1, and ADAB demonstrate higher reactivity, indicating that they are more likely to engage in chemical transformations.

We found that the inclusion of the water solution model led to a decrease in the energy levels of HOMO and LUMO, as well as a decrease in the energy gap between them ( $\Delta$ LUMO-HOMO). Therefore, we observed that the chemical potential and absolute hardness values also decreased compared to calculations performed in the gas phase. These findings suggest that the presence of a water solution in the calculations enhances the reactivity of the molecules under study. By considering the water solution model, there is a greater propensity for chemical reactions to occur. This highlights the importance of considering solvent effects when assessing the reactivity of molecules, as the water solution model can significantly influence their electronic properties and overall reactivity.

### Conclusion

The current research presented DFT calculations for molecules from azobenzene family. Specifically, we investigated 17 molecules using an innovative approach that incorporates DFT-D3 dispersion corrections, enhancing the accuracy of our results. Furthermore, we considered the effects of a water solvent by employing the polarizable continuum model (PCM), a technique that has not been applied in prior evaluations of these molecules.

Overall, adding the solvent model (water in our case) increases dipole moments for most molecules, with a stronger effect on highly polar compounds like SO<sub>2</sub>NH<sub>2</sub>AB, DO3, and DR1. In contrast, fluorinated molecules and some alkyl-substituted derivatives show relatively small changes, indicating that their dipole moments are less affected by solvation. The solvent generally enhances the contrast between *trans* and *cis* dipole moments, making the difference more pronounced in most cases.

The dipole moment difference between the *trans* and *cis* configurations was found to be lower in all considered molecules compared to azobenzene, except for ADAB. In the gas phase, ADAB exhibited a dipole moments difference of 4.89 Debye, whereas calculations including PCM yielded a difference of 6.89 Debye.

The relative difference in the dipole moment between the *trans* and *cis* configurations was found to be lower than for azobenzene for all considered molecules except for ADAB, for which the difference was obtained equal to 4.89 Debye in the gas phase and 6.89 Debye in calculations including PCM. Hence, materials incorporating this azobenzene derivative can be regarded as photoswitchable materials capable of transitioning between more and less hydrophilic states by transforming from the *cis* to *trans* configurations. This ability to switch wettability makes these materials promising candidates for various applications.

Moreover, ADAB molecule exhibited the largest mean and anisotropic polarizabilities, as well as the highest HOMO and LUMO energies. Also, ADAB molecules have shown to be the most reactive.

The highest negative difference in the dipole moments between *cis* and *trans* configurations was found for SO<sub>2</sub>NH<sub>2</sub>AB molecule. In the gas phase, this difference amounted to 4.55 Debye, while in the water solvent model it increased to 7.25 Debye. This finding suggests that this molecule holds promise for applica-

tions where the wettability of a surface needs to be altered under light irradiation, transitioning from a less hydrophilic state to a more hydrophilic state. Such materials could prove valuable in various fields requiring controllable surface properties.

These remarkable characteristics make the ADAB and  $\text{SO}_2\text{NH}_2\text{AB}$  molecules an intriguing subject for further exploration and potential applications.

Г. Адырбекова, П. Саидахметов, Р. Бурганова, И. Пиянзина,  
Г. Байман, Г. Баубекова, Д. Таюрский

### Тығыздықтың функционалдық теориясы шеңберінде сулануды өзгерту үшін азобензол туындыларын әлеуетті материалдар ретінде зерттеу

Зерттеуде тығыздықтың функционалдық теориясы (ТФТ) ылғалдылықты өзгертетін материалдар ретінде олардың әлеуетін бағалай отырып, 16 туынды азобензолдың қасиеттерін талдау үшін қолданылады. К. Ичимураның (2001) азобензолмен модификацияланған беттің сулануы туралы баяндамасынан шабыттана отырып, біз азобензолдың әртүрлі туындыларының *цис* және *транс*-конфигурациялары арасындағы молекулалық диполь моменттерінің өзгеруінен туындаған фотоизомеризацияның әсерін зерттедік. Бұл процесс бастапқы азобензол молекуласында полярлы емес молекуланы гидрофильді *цис* түріне айналдырады. Беттік қабаттың сулануын бақылау өнеркәсіптік, медициналық, микробиология, электроника және материалтану сияқты әртүрлі салаларда орасан зор әлеуетке ие. Осы бақылауды пайдалана отырып, біз инновациялық материалдарды жасау, функционалдылық пен тиімділікті арттыру әлеуетін аша аламыз. Бұл өнімнің өнімділігін жақсартуға, адгезияны жақсартуға және сұйықтықтарды өңдеу кезінде дәлдікке қол жеткізуге мүмкіндік береді. Дисперсиялық түзетілген DFT-D3 гибриді функционалды B3LYP және 6-31++G(d, p) базалық жиынтығын пайдаланып, зерттелген барлық молекулалардың құрылымдық, электронды және молекулалық аспектілері зерттелді, беттік қабаттың икемділігін басқаруға арналған перспективалы азот типті құрылымдар ұсынылды. Әлеуетті үміткер ретінде азобензолдың екі туындысы ұсынылған, олар *цис-транс* фотоизомерленуі кезінде бірі гидрофильділіктің жоғарылау бағытында, екіншісі қарама-қарсы бағытта түрлендірулерді көрсетеді.

*Кілт сөздер:* азобензол туындысы, ылғалдылыққа ауысу, фотоизомеризация, диполь моменттері, *cis-trans* конфигурациялары, DFT, B3LYP функционалдық, 6-31++G(d, p) базалық жинағы, фотоөткізгіш материалдар, гидрофильділік

Г. Адырбекова, П. Саидахметов, Р. Бурганова, И. Пиянзина,  
Г. Байман, Г. Баубекова, Д. Таюрский

### Исследование производных азобензола в рамках теории функционала плотности как потенциальные материалы для переключения смачиваемости

В этом исследовании теория функционала плотности (DFT) используется для анализа свойств 16 производных азобензола, оценивая их потенциал в качестве материалов, изменяющих смачиваемость. Вдохновленные докладом К. Ичимуры (2001) о смачиваемости поверхности, модифицированной азобензолом, мы изучаем влияние фотоизомеризации, вызванной изменением молекулярных дипольных моментов между *цис*- и *транс*-конфигурациями различных производных азобензола. В исходной молекуле азобензола этот процесс преобразует неполярную молекулу в более гидрофильную *цис*-форму. Контроль смачиваемости поверхности имеет большое значение в различных областях, таких как промышленность, медицина, микробиология, электроника и материаловедение. Используя этот контроль, мы можем раскрыть потенциал для создания инновационных материалов, повышения функциональности и эффективности. Он позволяет улучшить эксплуатационные характеристики продукта, улучшить адгезию и достичь точности при обращении с жидкостями. Нами изучены структурные, электронные и молекулярные аспекты всех исследованных молекул с помощью гибридного функционала B3LYP с дисперсионной коррекцией DFT-D3 и базисного набора 6-31++G(d, p), представив перспективные структуры азотистого типа для манипулирования смачиваемостью поверхности. Два производных азобензола выступают в качестве потенциальных кандидатов, демонстрируя трансформации в процессе *цис-транс* фотоизомеризации — одна в сторону увеличения гидрофильности, другая — в противоположном направлении.

*Ключевые слова:* производное азобензола, переключение смачиваемости, фотоизомеризация, дипольные моменты, *цис-транс* конфигурации, DFT, функционал B3LYP, базовый набор 6-31++G(d, p), фотопереключаемые материалы, гидрофильность

## References

- 1 Feng, C.L., Zhang, Y.J., Jin, J., Song, Y.L., Xie, L.Y., Qu, G.R., Jiang, L., & Zhu, D.B. (2001). Reversible wettability of photoresponsive fluorine-containing azobenzene polymer in Langmuir Blodgett films. *Langmuir*, 17(15), 4593–4597. <https://doi.org/10.1021/la010071r>
- 2 Miyauchi, M., Nakajima, A., Watanabe, T., & Hashimoto, K. (2002). Photocatalysis and photoinduced hydrophilicity of various metal oxide thin films. *Chemistry of Materials*, 14(6), 2812–2816. <https://doi.org/10.1021/cm020076p>
- 3 Ambrogio, M.W., Thomas, C.R., Zhao, Y.-L., Zink, J.I., & Stoddart, J.F. (2011). Mechanized silica nanoparticles: a new frontier in theranostic nanomedicine. *Accounts of chemical research*, 44(10), 903–913. <https://doi.org/10.1021/ar200018x>
- 4 Yu, X., Wang, Z., Jiang, Y., Shi, F., & Zhang, X. (2005). Reversible phresponsive surface: From superhydrophobicity to superhydrophilicity. *Advanced Materials*, 17(10), 1289–1293. <https://doi.org/10.1002/adma.200401646>
- 5 Minko, S., Muller, M., Motornov, M., Nitschke, M., Grundke, K., & Stamm, M. (2003). Two-level structured self-adaptive surfaces with reversibly tunable properties. *Journal of the American Chemical Society*, 125(13), 3896–3900. <https://doi.org/10.1021/ja0279693>
- 6 Wang, S., Song, Y., & Jiang, L. (2007). Photoresponsive surfaces with controllable wettability. *Journal of Photochemistry and Photobiology C: Photochemistry Reviews*, 8(1), 18–29. <https://doi.org/10.1016/j.jphotochemrev.2007.03.001>
- 7 Ichimura, K., Oh, S.-K., & Nakagawa, M. (2000). Light-driven motion of liquids on a photoresponsive surface. *Science*, 288(5471), 1624–1626. <https://doi.org/10.1126/science.288.5471.1624>
- 8 Von Seggern, N., Oehlsen, N., Moudrakovski, I., & Stegbauer, L. (2023). Photo-modulation of the mechanical properties and photo-actuation of chitosan-based thin films modified with an azobenzene-derivative. *Small*, 2308939. <https://doi.org/10.1002/sml.202308939>
- 9 Bricen˜o-Ahumada, Z., Tapia-Burgos, J.A., D'íaz-Leyva, P., Cadena-Aguilar, A., Garcia-Hernandez, F., & Kozina, A. (2023). Synthesis and cis-trans kinetics of an azobenzene-based molecular switch for light-responsive silica surfaces. *Journal of Molecular Liquids*, 390 (Part A), 122900. <https://doi.org/10.1016/j.molliq.2023.122900>
- 10 Sever, M., & Young, M.A. (2023). Isomerization kinetics of hydroxy-substituted azobenzenes using a modified commercial flash photolysis spectrometer. *Journal of Chemical Education*, 100(7), 2762–2769. <https://doi.org/10.1021/acs.jchemed.3c00200>
- 11 Aleotti, F., Petropoulos, V., Van Overeem, H., Pettini, M., Mancinelli, M., Pecorari, D., Maiuri, M., Medri, R., Mazzanti, A., & Preda, F., et al (2023). Engineering azobenzene derivatives to control the photoisomerization process. *The Journal of Physical Chemistry A*, 127(49), 10435–10449. <https://doi.org/10.1021/acs.jpca.3c06108>
- 12 Sıdır, İ., Gülseven Sıdır, Y., Berber, H., & Fausto, R. (2025). Solvatochromism and cis-trans isomerism in azobenzene-4-sulfonyl chloride. *Photochemical & Photobiological Sciences*, 1–15. <https://doi.org/10.1007/s43630-025-00684-0>
- 13 Sıdır, İ., Sıdır, Y.G., Berber, H., & Fausto, R. (2022). Solvato-, thermo- and photochromism in a new diazo diaromatic dye: 2-(p-tolyldiazenyl)naphthalen-1-amine. *Journal of Molecular Structure*, 1267, 133595. <https://doi.org/10.1016/j.molstruc.2022.133595>
- 14 Sıdır, İ., Kara, Y.E., Sıdır, Y.G., Berber, H., & Fausto, R. (2024). Reversal in solvatochromism, photochromism and thermochromism in a new bis-azo dye based on naphthalen-1-amine. *Journal of Photochemistry and Photobiology A: Chemistry*, 446, 115138. <https://doi.org/10.1016/j.jphotochem.2023.115138>
- 15 Ramírez-Rave, S., Ortega-Valdovinos, L.R., González-Castro, A.P., Yatsimirsky, A.K. (2024). Solvent and Temperature Dependencies of the Rates of Thermal Cis-to-Trans Isomerization of Tetra-(ortho) substituted 4-Aminoazobenzenes Containing 2,6-Dimethoxy Groups. *The Journal of Physical Chemistry B*, 128(31), 7639–7652. <https://doi.org/10.1021/acs.jpcc.4c02951>
- 16 Birla, H., Mir, S.H., Yadav, K., Halbritter, T., Heckel, A., Singh, J.K., & Gopakumar, T.G. (2023). Tuning the Switching Probability of Azobenzene Derivatives on Graphite Surface through Chemical Functions. *The Journal of Physical Chemistry C*, 127(34), 17039–17050. <https://doi.org/10.1021/acs.jpcc.3c02334>
- 17 Saito, N., Itoyama, S., Takahashi, R., Takahashi, Y., & Kondo, Y. (2021). Synthesis and surface activity of photoresponsive hybrid surfactants containing both fluorocarbon and hydrocarbon chains. *Journal of Colloid and Interface Science*, 582, 638–646. <https://doi.org/10.1016/j.jcis.2020.08.054>
- 18 Frisch, M.J., Trucks, G.W., Schlegel, H.B., Scuseria, G.E., Robb, M.A., Cheeseman, J.R., Scalmani, G., Barone, V., Petersson, G.A., Nakatsuji, H., Li, X., Caricato, M., Marenich, A.V., Bloino, J., Janesko, B.G., Gomperts, R., Mennucci, B., Hratchian, H.P., Ortiz, J.V., Izmaylov, A.F., Sonnenberg, J.L., Williams-Young, D., Ding, F., Lipparini, F., Egidi, F., Goings, J., Peng, B., Petrone, A., Henderson, T., Ranasinghe, D., Zakrzewski, V.G., Gao, J., Rega, N., Zheng, G., Liang, W., Hada, M., Ehara, M., Toyota, K., Fukuda, R., Hasegawa, J., Ishida, M., Nakajima, T., Honda, Y., Kitao, O., Nakai, H., Vreven, T., Throssell, K., Montgomery, J.A., Jr Peralta, J.E., Ogliaro, F., Bearpark, M.J., Heyd, J.J., Brothers, E.N., Kudin, K.N., Staroverov, V.N., Keith, T.A., Kobayashi, R., Normand, J., Raghavachari, K., Rendell, A.P., Burant, J.C., Iyengar, S.S., Tomasi, J., Cossi, M., Millam, J.M., Klene, M., Adamo, C., Cammi, R., Ochterski, J.W., Martin, R.L., Morokuma, K., Farkas, O., Foresman, J.B., & Fox, D.J. (2016). Gaussian 16 Revision C.01 Gaussian Inc. Wallingford CT.
- 19 Schlegel, H.B. (1982). Optimization of equilibrium geometries and transition structures. *Journal of Computational Chemistry*, 3(2), 214–218. <https://doi.org/10.1002/jcc.540030212>
- 20 Minisini, B., Fayet, G., Tsobnang, F., & Bardeau, J.F. (2007). Density functional theory characterization of 4-hydroxyazobenzene. *Journal of molecular modeling*, 13(12), 1227–1235. <https://doi.org/10.1007/s00894-007-0244-1>
- 21 Piyanzina, I., Minisini, B., Tayurskii, D., & Bardeau, F. (2015). *Journal of molecular modeling*, 21(34). DOI 10.1007/s00894-014-2540-x.

22 Mendoza-Huizar, L.H., & Rios-Reyes, C.H. (2011). Chemical reactivity of atrazine employing the fukui function. *Journal of the Mexican Chemical Society*, 55(3), 142–147. <https://doi.org/10.29356/jmcs.v55i3.812>

23 Zhan, C-G., Nichols, J.A., & Dixon, D.A. (2003). Ionization potential, electron affinity, electronegativity, hardness, and electron excitation energy: Molecular properties from density functional theory orbital energies. *The Journal of Physical Chemistry A*, 107(20), 4184–4195. <https://doi.org/10.1021/jp0225774>

### Information about the authors

**Adyrbekova, Gulmira** — Associate professor (Chemistry), M. Auezov South Kazakhstan University, Shymkent, Kazakhstan; e-mail: [adyrbekova.gulmira@mail.ru](mailto:adyrbekova.gulmira@mail.ru); ORCID ID: <https://orcid.org/0000-0003-4411-7713>

**Saidakhmetov, Pulat** (*corresponding author*) — Candidate of Science (Physics), Assistant professor, Department of Physics, M. Auezov South Kazakhstan University, Shymkent, Kazakhstan; e-mail: [timpf\\_ukgu@mail.ru](mailto:timpf_ukgu@mail.ru); ORCID ID: <https://orcid.org/0000-0002-9146-047X>

**Burganova, Regina** — Institute of Physics, Kazan Federal University, Kremlyovskaya St. 18, Kazan, 420008, Tatarstan, Russia; e-mail: [bur.regina@gmail.com](mailto:bur.regina@gmail.com); ORCID ID: <https://orcid.org/0000-0002-5985-265X>

**Irina, Piyanzina** — PhD senior research fellow, Institute of Physics, Kazan Federal University, Kremlyovskaya St. 18, Kazan, 420008, Tatarstan, Russia; e-mail: [i.piyanzina@gmail.com](mailto:i.piyanzina@gmail.com); ORCID ID: <https://orcid.org/0000-0003-4251-9196>

**Baiman, Gulzagira** — Senior Lecturer, Department of Physics, M. Auezov South Kazakhstan University, Shymkent, Kazakhstan; e-mail: [bgb\\_zht@mail.ru](mailto:bgb_zht@mail.ru); ORCID ID: <https://orcid.org/0000-0003-4250-842X>

**Baubekova, Gulnara** — Senior Lecturer, Department of Physics, M. Auezov South Kazakhstan University, Shymkent, Kazakhstan; e-mail: [baubekova83@mail.ru](mailto:baubekova83@mail.ru); ORCID ID: <https://orcid.org/0009-0006-5638-0470>

**Tayurskii, Dmitrii** — Doctor of Science (Physics and mathematics), Professor, Vice-rector, Kazan Federal University, Kremlyovskaya St. 18, Kazan, Russia; e-mail: [Dmitry.Tayurskii@kpfu.ru](mailto:Dmitry.Tayurskii@kpfu.ru); ORCID ID: <https://orcid.org/0000-0001-6106-7581>